Reaktor

p-ISSN 0852 – 0798
e-ISSN 2407 – 5973

Website: http://ejournal.undip.ac.id/index.php/reaktor/

Reaktor, Vol. 23 No. 1, April Year 2023, pp. 27-37

Chitosan-Modified Fly Ash/Kaolin Ceramic Membrane for Enhancing FOG-Water Separation Performance

Eny Apriyanti[1,2*)], Heru Susanto[1,3)], dan I Nyoman Widiasa[1,3)]

[1)]Department of Chemical Engineering, Faculty of Engineering, Universitas Diponegoro, Indonesia
Jl. Prof. Soedarto SH Tembalang Semarang
Telp./Fax. (024)7460058 / (024)76480675
[2)]Laboratorium Teknologi Material, UPT Laboratorium Terpadu Universitas Diponegoro
Jl. Prof. Soedarto SH Tembalang Semarang
Telp./Fax. (024)7460055/(024)7645567
[3)]Membrane Research Center (MeR-C), UPT Laboratorium Terpadu Universitas Diponegoro, Indonesia
Jl. Prof. Soedarto SH Tembalang Semarang
Telp./Fax.: (024)7460057/(024)7465879
Corresponding author: enyapriyanti@ymail.com

(Received: 14 May 2023; Published: 30 Mei 2023)

Abstract

Ceramic membranes with efficient construction can save costs and simplify the wastewater treatment process. Ceramic membranes are potentially used in wastewater treatment due to their high mechanical stability however they possess a low molecular separation rate. Thus, this study aims to develop a low-cost ceramic membrane with high separation efficiency by chitosan surface-coating. The price of raw materials and the amount of energy used during the sintering process are the two key factors that affect the final cost of ceramic membranes. This work used kaolin and fly ash recovered from power plants as the support ceramic membrane and chitosan as the selective layer of composite ceramic membranes. Rigid alumina particles were added to the supports to bring them into alignment with the sintering temperature of the fly ash/kaolin support. Additionally, the chitosan layer coating increased the supports' bending strength. By simple surface coating, chitosan with different molecular weights were spread over the fly ash/kaolin supports. The membrane average pore size radius and porosity were 20 nm and 49%, respectively. The oil removal rate was over 99.8% and the stable permeate flux was close to 20.5 $Lm^{-2}h^{-1}$ when treating oil-water emulsions with 400 mg/L oil content. This is most likely because of the super-hydrophilic performance of kaolin and the electrostatic repulsion between the membrane and oil droplets. The fabricated membranes also demonstrated high antifouling performance by enhancing FRR up to 88% and significantly reduced the reversible fouling ratio. This study suggests that modified membrane has great potential for practical application in oily wastewater treatment.

Keywords: *ceramic membrane; chitosan; fly-ash; fouling, kaolin; wastewater*

How to Cite This Article: Apriyanti, E., Susanto, H., dan Widiasa, I. N., (2023), Chitosan-Modified Fly Ash/Kaolin Ceramic Membrane for Enhancing FOG-Water Separation Performance, Reaktor, 23 (1), 27-37, https://doi.org/10.14710/reaktor. 23. 1. 27-37

INTRODUCTION

The sustainable development of society depends on the sustainable supply of clean water. Water scarcity due to water contamination is a worldwide problem that threatens human activities (Chen et al., 2021). Water security is considered to

have an important role in the sustainable food security of countries especially those with limited natural water resources (Al-Thani & Yasseen, 2020). The degradation of clean water resources is reported as the effects of agriculture, industrial, and domestic activities (Kadam et al., 2020). Domestic wastewater is one of the most potential wastewater sources that contaminate surface water. The production of wastewater from households is approximately 135 L per person per day (Drozdova et al., 2019). This condition is exacerbated by inappropriate domestic wastewater treatment, especially in developing countries that have not implemented integrated wastewater treatment plants (IWWTP) for domestic activities. The discharge of untreated domestic wastewater intothe environmental body has been studied to have severe damage to the aquatic life and potentially degrades the quality of ground water (He & Li, 2020). Domestic water is usually categorized as two types i.e., black water and grey water. Black water is the discharge wastewater from toilets that contains high organic content. Grey water is all other wastewater exfrom the toilets including sink, shower, and laundry. Grey water contains relatively low organic compounds however some persistent and emerging contaminants are often found in the wastewater such as surfactants, heavy metals, and fats, oil & grease (FOG). Typical characteristic of domestic wastewater contains biochemical oxygen demand (BOD) of 125 – 400 mg/L^{-1}, chemical oxygen demand (COD) of 230 – 780 mg.L^{-1} (Widyarani et al., 2022), total nitrogenic compounds of 20 – 35 mg.L^{-1} (Y. Li et al., 2017), surfactants of 10 – 20 mg.L^{-1} (Dereszewska et al., 2015), heavy metals of 0.1 – 2 mg.L^{-1} (Bakare & Adeyinka, 2022), and FOG of approximately 10 – 150 mg.L^{-1} (Pastore et al., 2015). Eljaiek-Urzola et al. (2019) reported that presence of FOG in water caused devastating physical effects such as coating animals and plants with oil and suffocating them by oxygen depletion and blocks enough sunlight to penetrate the water, considered as toxic and generating toxic products, destroyed animals food supplies, breeding, and habitats, and producean unpleasant odor. FOG also potentially blocks the sewage pipes when it solidifies. The built-up FOG in pipes increased the maintenance costs. Khozanah et al. (2021) have found high concentration of FOG in seawater and sediment of Jakarta Bay, Indonesia up to 258 mg.L^{-1} and 18 mg.kg^{-1}, respectively due to the accumulation of discharged wastewater from the cargo and domestic activities. These concentrations are higher than the sea water quality accordingthe to Decree of Indonesia Environment Ministry and Australian - New Zealand Environment and Conservation Council (ANZECC). Therefore, upstream prevention of FOG contamination by a proper wastewater management is essentially required to prevent further environmental damage. Furthermore, grey water treatment into clean water can be a part of the water conservation to support sustainable development goals (SDGs) number 6.

Ceramic membrane-based separation is considered as an effective method for separating oil in water emulsion (Liu et al., 2023). There are several advantages of ceramic membrane over polymeric membrane i.e. higher mechanical stability from the action of chemical cleaning, chemical robustness of ceramic membranes permits more aggressive chemical cleaning, high porosity leading on higher permeate flux, microbiological resistance, and longer lifetime (Siskens, 1996). Even though there is growing interest in basic research and industrial uses for ceramic membranes, their ability to be used in broader and larger-scale applications is severely constrained by their high capital cost relative to polymeric membranes with equivalent efficiency. For comparison, the price of ceramic membrane with 125 L.$m^{-2}h^{-1}$ (LMH) permeate flux is approximately ~$175 USD per m^2 while polymeric membrane with similar performance is ~$35 USD per m^2. Therefore, academic groups are progressively focusing on different methods of reducing cost and boosting efficiency, including the development of low-cost ceramic membranes, innovative production and processing methods, and numerous prospective performance-enhanced coupling schemes (Dong et al., 2022).

Conventional ceramic membranes are typically made of Al_2O_3, ZrO_2, TiO_2, and SiC, which all belong to the group of expensive inorganic materials. The membrane preparation method also requires multi-step dip-coating on large pore size support that each layer consists of once dip-coating, drying and sintering process, which increases the costs. Therefore, many researchers have developed novel ceramic membrane materials from both low-cost raw material and preparationmethodsd. There is a growing interest in the fabrication and application of low-cost ceramic membranes based on naturally occurring raw materials and waste products. Saini et al. (2019) proposed kaolin-based ceramic membrane for textile industry wastewater treatment where the results showed high water permeability up to 1376 LMH with considerable removal of COD and BOD of 39%. Mouiya et al. (2019) developed ceramic membrane from natural clay and banana peel powder. The performance evaluation has shown that the membrane reached remarkable performance of 550 LMH permeate flux and ~86% COD rejection. The banana peel powder was used as natural pore-forming agent in the membrane preparation process. Other waste bio-material such as fish bone was also utilized as ceramic membrane with high separation efficiency up to 99.9% of heavy metal removal and high flux of ~250 LMH (Hubadillah et al., 2023). The utilization of fly ash waste as ceramic membrane raw material has shown potential performance of 92% oil removal with flexural strength of ~38 MPa (Das et al., 2020). For improving the oil-water separation efficiency as well as improving the mechanical properties, Zou et al. combined kaolin and fly ash by spraying kaolin suspension onto alumina-fly ash support resulted in

high permeate flux of ~530 LMH and enhanced oil rejection up to ~98%. In this study, natural kaolin and fly ash was combined as membrane support. For creating the selective layer, chitosan layer was added by dip-coating method. Bat-Amgalan et al. (2022) reported that the chitosan coating on ceramic membrane enhanced membrane properties such as mechanical stability, ultrafine structure, improved hydrophilicity, and higher solute rejection. However, the chitosan layer on ceramic membrane is potentially damaged due to hydrodynamic shear force and low interaction between ceramic support and selective layer. To overcome those issues, TiO_2 was incorporated into ceramic support to increase the interfacial interaction of ceramic membrane support with chitosan layer. The crosslinking using glutaraldehyde was also performed to prevent the swelling of selective layer due to hydrophilic nature of chitosan.

In this work, a simply one-step co-sintering method was performed to prepare kaolin/fly ash composite ceramic support. TiO_2 nanoparticles were incorporated into ceramic membrane support via dip-coating and followed by membrane drying and sintering. The selective layer was prepared by dip-coating into chitosan solution and followed by crosslinking process using glutaraldehyde. The objectives of this study are to develop low-cost ceramic membrane with high separation efficiency towards oil-water emulsion and investigate the effect chitosan coating with different molecular weights on the membrane characteristics and performances. The physicochemical properties of the fabricated membrane were investigated as well as its performance for separating FOG in water. The raw materials used in this study are relatively inexpensive and bio-based material that was expected to produce low-cost ceramic membrane with higher performance thereby more affordable for industrial application.

MATERIALS AND METHODS

Materials

The materials used for ceramic membrane support preparation were fly ash from local power plant Paiton Energy Ltd. (Probolinggo, Indonesia), natural kaolin powder from Brataco Chemical Ltd. (Semarang, Indonesia), carboxymethyl cellulose (CMC) and magnesium sulfate were from Merck (Singapore Science Park, Singapore). The membrane modifiers such as titanium dioxide, alumina, polyethylene glycol (PEG), and sodium citrate were supplied from Sigma Aldrich (Pasir Panjang, Singapore). Chitosan low molecular weight (50 – 190 kDa), medium molecular weight (190 – 300 kDa), and high molecular weight (310 – 375 kDa) as coating agent were purchased from Sigma Aldrich (Pasir Panjang, Singapore). Vegetable oil as synthetic wastewater preparation was purchased locally. Other chemicals for analysis and characterization were pro-analyst grade from Merck (Singapore Science Park, Singapore). Deionized water was used for all chemical solutions preparation.

Preparation of fly ash/kaolin ceramic membrane support

Ceramic membrane raw materials such as fly ash, kaolin, and alumina were sieved with 200 mesh sieving devices. The mass ratio of fly ash, kaolin, and alumina were 7:10.4:1, respectively. Appropriate amount of 1 wt.% of CMC, 1 wt.% of sodium citrate, 2 wt.% of PEG, and 1 wt.% of $MgSO_4$ were added as binding agent and reinforcing materials. 3 wt.% of deionized water was added and subsequently stirred at 600 rpm for 60 min to form homogeneous printing slurry. The proto-membrane slurry was then left at room temperature for 30 min for aging process. The slurry was compacted under 150 MPa in rectangular and cylindrical mold forming flat disks with diameter of 50 mm and thickness of 2 mm.

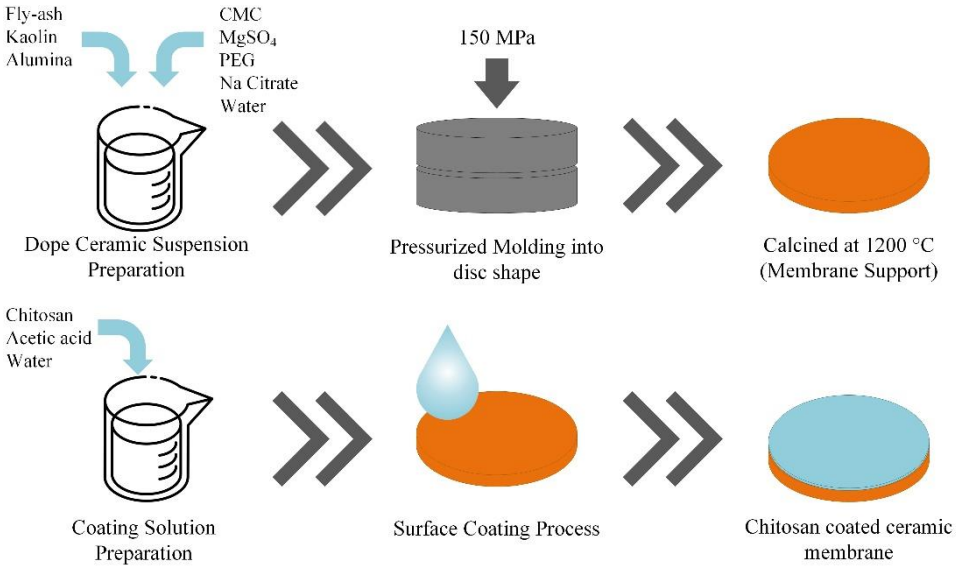

Figure 1. Schematic diagram of ceramic membrane fabrication

The molded ceramic membrane support was dried at 250 °C for an hour to remove the water content as well as the removal of volatile organic compound from wastewater. Finally, the casted membrane support was calcined at 1200 °C for 7 h.

Membrane modification using chitosan

Prior to chitosan modification, the ceramic membrane support as prepared in the previous section was impregnated by TiO_2 nanoparticles. Approximately 1 gr of TiO_2 was dissolved into 100 mL of 0.1 M NaOH solution than continuously stirred for 2 h. the ceramic membrane support was then immersed into the TiO_2 solution for 1 h and subsequently sintered at temperature of 1100 °C for 7 h. For chitosan modification, the 2 wt.% solutions of low molecular weight chitosan (LC), medium molecular weight chitosan (MC), and high molecular weight chitosan (HC) were prepared in 1 wt.% of acetic acid solution. Then, 5 mL of chitosan solution was poured onto ceramic membrane support and cast using fia lm applicator device with thickness gap of 200 µm. The casted membrane was then immersed in a coagulation bath containing deionized water at room temperature for phase separation. The prepared membrane was washed to remove solvent residue and the membrane was dried at ambient temperature for 1 h then 24 h at 40 °C for complete drying process. Low, medium, and high molecular weighchitosan-coateded membranes were then labeled as LCM, MCM, and HCM, respectively. The fabrication process is simply illustrated in Figure 1.

Membrane characterizations

The surface morphology of the ceramic membrane was observed using scanning electron microscope (SEM, JEOL Series, JSM-6510-LA, Japan). The thermal stability of the membrane was investigated using thermal gravimetric analysis (TGA, Hitachi STA200RV, Japan). The mechanical strength of membranes was measured by a bending method at a rate of 0.5 mm.min^{-1} and distance of 3.0 cm. Phase identification of the prepared membranewasre carried out using an X-ray powder diffractometer (XRD, Shimadzu Japan) using CuKα = 1.5419 Å, 40 kV, 40 mA radiation in the range of 2θ from 15° - 90° with an increment of 0.01°.

The porosity (ε) of the ceramic membranes was determined using Archimedes principle as reported by previous study (Jafari et al., 2021). The moisture presence in the membranes was eliminated by maintaining the membrane in the oven at 80 °C for 4 h then the weight of dried membranes was measured (w_{dry}). The membranes were then immersed in the deionized water for 24 h then the excess water on the membrane surface was wiped using filter paper. Then, the weight of wet membranes was measured (w_{wet}).

The porosity of the membrane can be calculated by the following equation.

$$\varepsilon(\%) = \left[\frac{\frac{(w_{wet}-w_{dry})}{\rho_w}}{\pi R^2 \delta}\right] \times 100\% \qquad (1)$$

Where R, ρ_w, and δ are membrane radius (cm), membrane thickness (cm), and density of pure water at 25 °C (0.9970 g.cm^{-3}).

The membrane pore size radius (r_m) was estimated using empirical correlation equation of fluid flow in porous medium developed by Guerout-Elford-Ferry (Kusworo et al., 2021) as follow.

$$r_m = \sqrt{\frac{(2.9-1.75\varepsilon)8\mu\delta J}{\varepsilon TMP}} \qquad (2)$$

Where µ, J, and TMP are pure water viscosity at 25 °C (0.00089 Pa.s), pure water permeate flux (m^3.m^{-2}.s^{-1}), and trans membrane pressure (Pa).

Membrane Performance Evaluation

The ceramic membranes were prepared to treat synthetic oil-water (O/W) emulsion in this study with the concentration of vegetable oil was 400 mg/L^{-1} and 0.12 g. L^{-1} of sodium dodecyl sulfonate (SDS) as emulsifier. The emulsification of synthetic wastewater was performed under continuous stirring at 1000 rpm for 15 min. The performance evaluation of the membrane also performed filtration experiment using real domestic wastewater obtained from wastewater sewage in Semarang, Indonesia. The membrane filtration test was performed using a cross-flow membrane filtration device with trans membrane pressure of 5 bar. The volume of permeate was collected and periodically measured for the volume to determine the permeate flux value using the following equation.

$$J = \frac{V}{A.t} \qquad (3)$$

Where J is the permeate flux (L.m^{-2}.h^{-1}), V is the collected permeate water volume (L), A is the effective membrane area (0.00196 m^2), and t is the filtration time (h).

The oil removal efficiency was determined by measuring the concentration of oil in permeate water using UV-Vis spectrophotometer at a wavelength of 277 nm (Ghanbari et al., 2018). Then, the oil rejection (R) was calculated using equation as follow.

$$R(\%) = \left[\frac{C_f - C_p}{C_f}\right] \times 100\% \quad (4)$$

C_f and C_p represent the oil concentration in water of feed and permeate, respectively.

Membrane Fouling Analysis

The short-term organic fouling analysis was conducted in a cross-flow filtration system where both permeate and retentate were recycled to the feed water to maintain a constant water quality. The organic fouling experiments were performed using humic acid (HA) solution with a concentration of 10 mg. L^{-1} as feed model. The filtration was run at 5 bar trans membrane pressure for 4 h and the permeate water was periodically collected and weighed. After the filtration, the membrane was cleaned using deionized water (forward and surface flushing) to removthe e attached foulant. The cleaned membrane was then used to measure the permeate water flux at the same operating condition. From this experiment, the flux

recovery ratio (*FRR*), total fouling ratio (R_t), reversible fouling ratio (R_r), and irreversible fouling ratio (R_{ir}) were calculated as follows (C. Li et al., 2019):

$$FRR(\%) = \frac{J_1}{J_0} \times 100\% \quad (5)$$

$$R_t(\%) = \left(1 - \frac{J_2}{J_0}\right) \times 100\% \quad (6)$$

$$R_{ir}(\%) = \left(\frac{J_1 - J_2}{J_0}\right) \times 100\% \quad (7)$$

$$R_r(\%) = \left(\frac{J_0 - J_1}{J_0}\right) \times 100\% \quad (8)$$

Where FRR is the flux recovery ratio, J_0, J_1, J_2 are the initial permeate flux, permeate flux after membrane cleaning, and permeate flux after 5 h filtration of HA solution.

RESULTS AND DISCUSSIONS

Membrane Morphology using SEM

Membrane surface morphologies are important characteristics for membrane separation and permeation performances. Figure 2 shows the SEM images of membrane surface with different chitosan molecular weight coating modification.

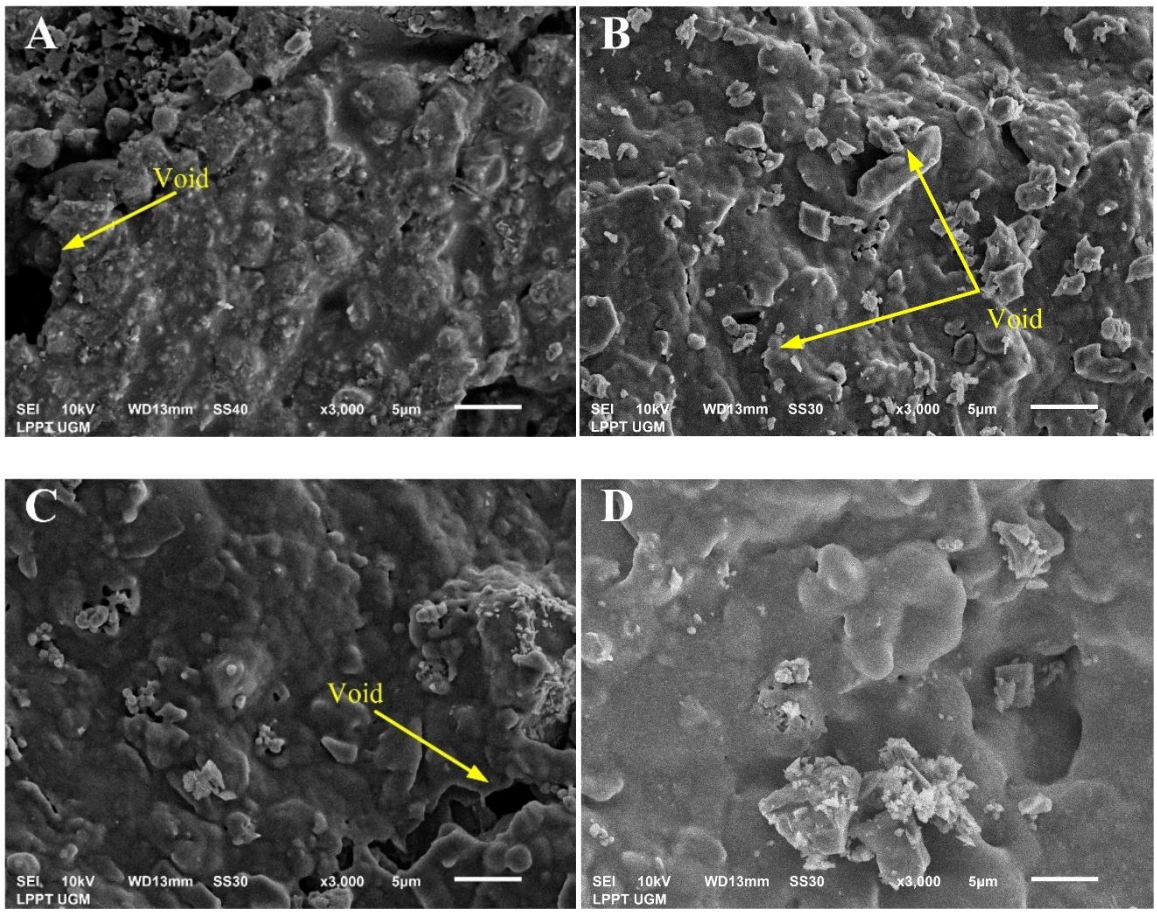

Figure 2. SEM images of membrane surface of (A) uncoated ceramic membrane, (B) LCM, (C) MCM, (D) HCM

The sintering temperature is the key factor in resulting the rigid membrane support of the fly ash/kaolin (Saini et al., 2019). Based on the SEM images, there is no crack observed on the membrane surface indicating that the sintering temperature is appropriate for fly ash/kaolin mixture. As shown in the Figure 2, the sintered ceramic membrane surface with different molecular weight of chitosan coating has influenced the membrane surface topography. The uncoated membrane was shown in Figure 2A with typical rough surface. Unselective voids were also observed indicating the uncoated membrane has low separation performance. Figure 2B shows low-molecular weight chitosan coated membrane (LCM). Unselective voids are observedon the membrane surface that may lead on lower separation performance. For higher molecular weight of chitosan, the number of voids decreases as the pore size also significantly decreases. It could be due to the higher molecular weight of chitosan also provides higher packing density of the chitosan thus effectively cover the membrane surface. Bat-Amgalan et al. (2022) also confirmed that successful chitosan coating on the ceramic membrane has effectively eliminate the unselective voids due to membrane cracking. Our previous study has revealed that fly ash containing ceramic membrane support with high Al/Si content might tightened the porous structure thereby inhibiting the membrane permeation rate during filtration (Apriyanti et al., 2018). This kind of membrane structure will increase the selectivity towards pollutant in wastewater filtration process.

FTIR Analysis Results

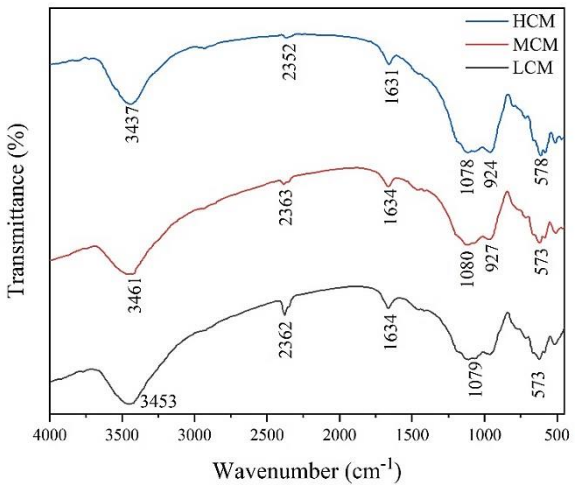

Figure 3. FTIR spectra of fabricated membranes

FTIR analysis results for three membranes with chitosan modification which have different molecular weights are depicted in Figure 3. Overall, the FTIR spectrum shown by the three membranes has a consistent IR transmittance profile with a peak at a wavelength of around 3450 cm^{-1} indicating the presence of IR adsorption by the amine group (NH_2) belonging to the chitosan molecule (Fatoni et al., 2018). Furthermore, the weak peak at 2360 cm^{-1} indicates the presence of silane groups (Si) originating from fly ash which is the raw material for supporting the membrane (Fauzi et al., 2016). The peak at 1634 cm^{-1} also indicates the presence of IR adsorption by the amine group (NH_2) of the chitosan molecule. The IR adsorption band at a wavelength of ~1080 cm^{-1} indicates the vibration of the Si-O groups present in kaolin and fly ash. Similar results were also reported by Kyriakogona et al. (2017) where the FTIR profile of calcined kaolin shows a strong IR adsorption at a wavelength of around 1079 cm^{-1}. The weak peak in the fingerprint area (finger print) at around 573 cm^{-1} indicates the presence of vibrations from the Al-O-Al groups of alumina, kaolin, and fly ash.

XRD Analysis Results

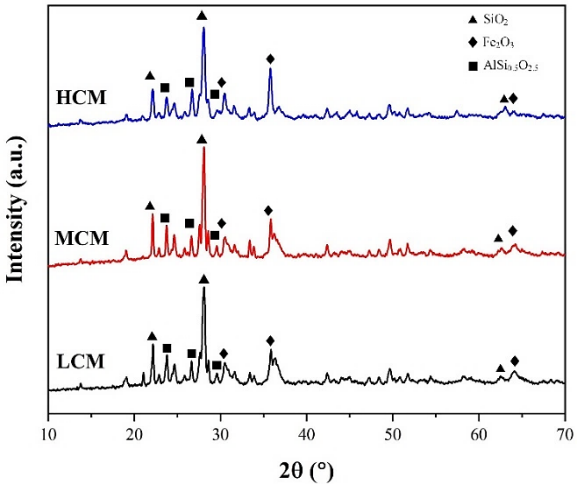

Figure 4. XRD pattern of membrane with different chitosan coatings

The X-ray diffraction pattern of three different chitosan coated ceramic membranes are presented in Figure 4. The observation of peaks and patterns in the XRD graphs reveal that the inorganic mixture originally consisted of kaolinite, alumina, and fly ash as the main components. The kaolinite pattern was strongly identified with high intensity diffraction at 2θ at 27.8° (JCPDS 00-005-0143). Agarwal et al. (2020) also found the similar XRD pattern for membrane with kaolinite as main composition. The chemical identification showed that SiO_2 in quartz phase (JCPDS 00-046-1045) is the highest component (65.66 wt%) followed with α-Al_2O_3 (JCPDS 050-0741) (27.84 wt%) with trace of other minerals such as hematite Fe_2O_3 (JCPDS 98-005-3677) (0.39 wt%). The sintering process at temperature more than 750 °C caused de-hydroxylation of kaolinite to form metakaolinite identified by the reduction of peak at 2θ at 27.8° and further metakaolinite decomposed to form mullite (Guo et al., 2007). It is clearly seen that the phase transformation due to chitosan coating does not cause any significant phase structural changes. The characteristic peak of chitosan is single sharp peak at

2θ = 20.9°. however, this characteristic peak of chitosan is not detected in the XRD pattern. It might arise from the fact that chitosan is amorphous material with low diffraction intensity.

Thermal Stability Analysis Results

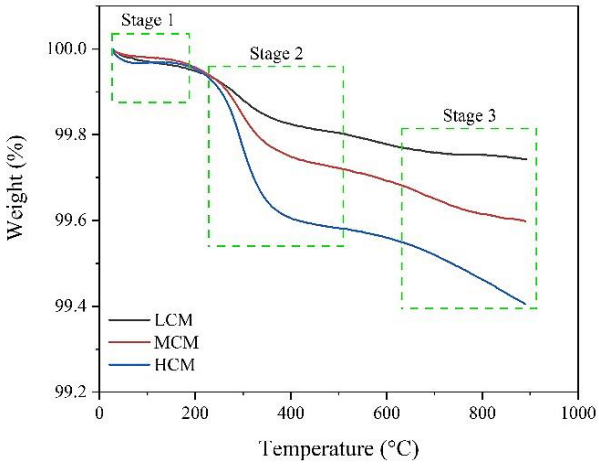

Figure 5. typical TGA profile of chitosan-modified ceramic membrane

TGA test results for three ceramic membrane samples are presented in Figure 5. The decrease in mass with increasing temperature for the three membrane samples has the same profile. From the results of more in-depth observations, there are three stages of thermal degradation in ceramic membrane samples. Stage 1 decreases in mass in the temperature range between 80 – 200 °C, this decrease is probably caused by the evaporation of water molecules contained in the pores of the membrane. Stage 2 is a sharp reduction in the temperature range of 200 – 500 °C, degradation of carbon residue from additives such as CMC in the ceramic membrane manufacturing process and the dehydroxylation of kaolin to form metakaolin and mullite (Agarwal et al., 2020). Stage 3 occurs at a temperature of 600 – 900 °C where the decomposition of remaining carbon from organic additives continues but occurs slowly so that the profile shows a gentle downward curve. Of the three ceramic membrane samples, the membrane with low molecular weight chitosan coating (LCM) had the best thermal stability with a weight loss percentage of 0.25%, then the membrane with medium molecular weight chitosan coating (MCM) with a weight loss percentage of 0.4% and the ceramic membrane with high molecular weight chitosan coating (HCM) showed the largest percentage of weight loss with a value of 0.6%. The largest mass decrease shown by the membrane with high molecular weight chitosan coating is probably caused by the greater of packing density of HC thus degraded in high temperature. Moreover, HC has characteristic to adsorb more water vapor. This can be seen in the profile of TGA stage 1, the decrease in mass for HCM shows the largest amount of water evaporation. However, all prepared ceramic membranes have good thermal stability where at 900 °C the mass of the membrane still remains 99.40 – 99.75%.

Porosity, Pore Size, and Mechanical Strength

The porosity and pore size radius are key parameters that driving the permeability and selectivity of the membrane during filtration process. The porosity characteristic is strongly influenced by raw materials, fabrication process, and post-modification. The metasilicate crystals contained in membrane support leads to fusion further densification of the structures that enhances the binding characteristics of the membrane (Agarwal et al., 2020). The porosity and pore size radius of the membranes are presented in the Table 1. All membranes have similar porosity value, it could be due to the formula of the membrane support is same. The proportion of kaolin and fly ash affect the porosity structure of the membrane. Hubadillah et al. (2016) reported that higher kaolin content helps to densify the membrane structure. The uncoated membrane (M0) showed porosity and pore size radius of 50.02% and 26.41 nm, respectively. After the membrane was coated by chitosan with different molecular weight, the porosity and pore size radius significantly decrease. The lowest porosity was obtained by LCM of 48.94%. It could be due to the lower molecular weight of chitosan has lower viscosity (Kapadnis et al., 2019) thus the coating solution has filled the membrane voids. Otherwise, the higher molecular weight of chitosan has higher rheological properties that maintained on the membrane surface. The pore radius decreases with the increase of molecular weight of chitosan. As mentioned in the previous section, higher molecular weight of chitosan has higher packing density that that of low molecular weight chitosan. The tensile strength of the membrane significantly improved with chitosan coating from 84.72 MPa to 112.47 MPa. The presence of chitosan molecule on the membrane surface has strengthen the membrane integrity despite receiving high energy load. Kotobuki et al. (2021) found that the application of organic polymer into inorganic ceramic membrane has demonstrated higher tensile strength.

Table 1. Porosity, pore size radius, and tensile strength of the fabricated ceramic membranes

Membrane	Porosity, ε (%)	Pore radius, r_m (nm)	Tensile Strength (MPa)
M0	50.02	26.41	84.72
LCM	48.94	20.98	96.31
MCM	49.32	20.13	109.80
HCM	49.71	15.84	112.47

These experimental results suggest that the fabricated membranes have improved pore-structure properties that beneficial for filtration experiment of oil-water separation. The size of free-oil in water is around 150 µm, dispersed oil is in the range of 20 – 150 µm, and

emulsified oil is <20 µm. ultrafiltration (UF) membrane with pore size of 10 – 100 nm is considered as appropriate membrane for separating oil droplet (<10 µm) with high separation efficiency.

Performance in Oil/Water Separation

The performance of fabricated membrane is evaluated by measuring the permeate flux and oil rejection. Figure 6(a) shows the variation of permeate flux with different coating treatment for oil-water filtration. The unmodified membrane (M0) showed severe flux decline from 65 $L.m^{-2}.h^{-1}$ to ~50 $L.m^{-2}.h^{-1}$. This flux decline could be attributed to the deposition oil droplet within membrane pores as well as membrane surface. Due to the deposition, the resistance to the permeate flux grows with the time operation. All modified membranes showed lower permeate fluxes due to the chitosan coating increases the hydraulic resistance of the membrane. as presented in Table 1, the pore sizes of the modified membranes are narrower than that of unmodified membrane. despite the permeate fluxes are lower, the modified membranes (LCM, MCM, HCM) showed relatively steady profile indicating that the chitosan coating helps to prevent oil deposition. It could be due to the hydrophilic nature of chitosan. The hydrophilic surface can effectively prevent the oil deposition and the consequent blocking of pores (Kusworo et al., 2017). HCM exhibits the lowest permeate flux due to the high-molecular chitosan has higher packing density thus increasing the membrane resistance. Furthermore, according to the pore size measurement, HCM shows the smallest pore size diameter leading on lowest permeate flux. Another parameter for performance evaluation is pollutant rejection as presented in Figure 6(b). An enhancement of oil rejection was observed of the modified membrane from ~88% to ~99% rejection efficiencies. Among the fabricated membranes, there is no significant difference of oil rejection. it could be due to the average pore size of the membranes are around 15 – 20 nm. UF membranes with the pore size of 10 – 100 nm are the most effective and efficient for oil rejection. Chitosan coating creates narrow pore size and provide hydrophilic layer thus enhance the oil rejection via size exclusion and Donnan's exclusion mechanisms. Size exclusion mechanism is the common separation mechanism in membrane where the solutes with a larger size than the pore size of the membrane are retained. Donnan's exclusion mechanism is an exclusion mechanism in membrane as the effect of charge repulsion force between membrane and solutes. The performance evaluation demonstrated that the modified membrane has excellent oil-water separation efficiency with moderate permeate flux. It suggests the potential of practical application in the large scale especially for treating oily wastewater.

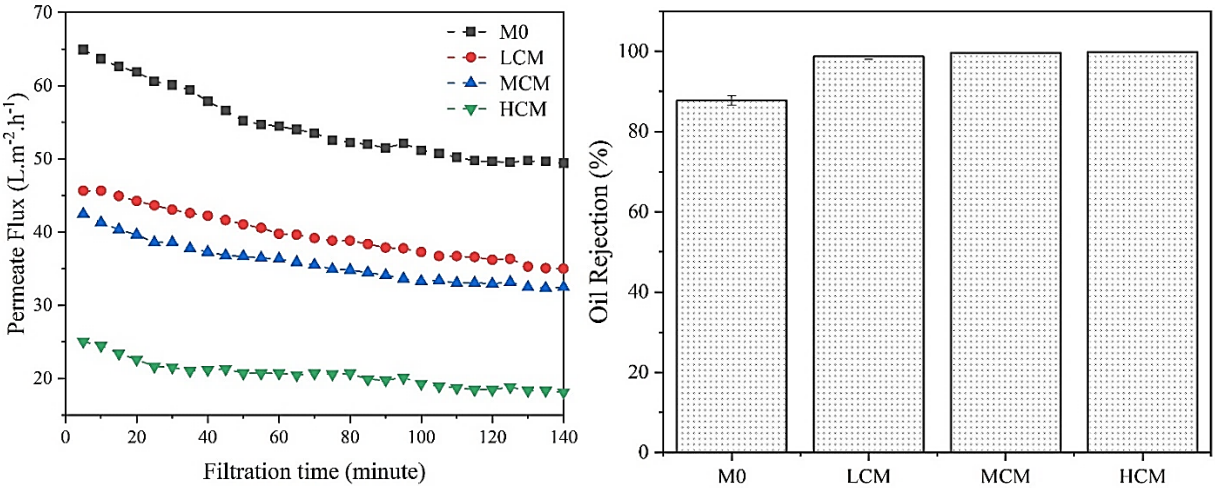

(a) (b)

Figure 6. performance evaluation of ceramic membranes (a) permeates flux profile (b) oil rejection efficiencies

Fouling Analysis

Fouling is the major obstacle in the membrane application that decline the permeate flux of the membrane during filtration processes. There are four fouling mechanism namely complete pore blocking, intermediate pore blocking, standard pore blocking, and cake filtration. Fouling can also be either reversible or irreversible in almost all membrane operation. In general, reversible fouling is attributed to the concentration polarization and deposition of the rejected substances on the membrane surface. This type of fouling is easily removed by hydraulic cleaning. The irreversible fouling is from internal blockage of the pores by organic or inorganic foulants (Bousbih et al., 2021). This type of fouling requires chemical cleaning to remove the foulant completely. The evaluation of fouling growth in this experiment was performed by measuring the flux ratio before and after cleaning compared with pure water flux. The results of flux ratios are demonstrated in the Figure 7 bellow.

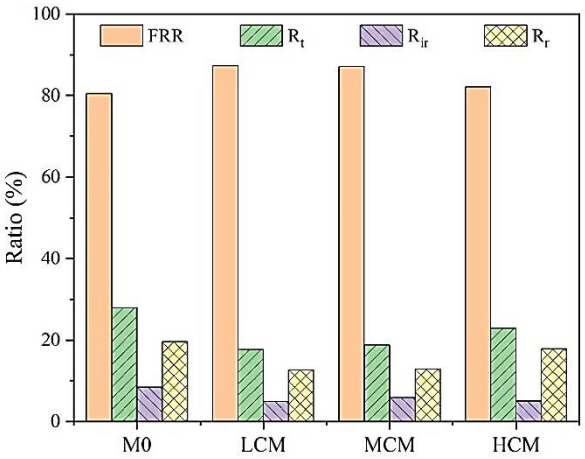

Figure 7. Flux recovery ratio (FRR) and fouling ratios of the fabricated membranes

Fouling growth can be evaluated by measuring the flux recovery ratio (FRR) of the prepared membranes. All modified membranes have shown higher FRR value than that of unmodified membrane. the FRR of the unmodified membrane is ~80% and the FRR of modified membranes are ranging from 85 to 88%. It means that the filtration performance of the prepared membranes was enhanced when they were exposed to the oil emulsion solution. Among the modified ceramic membrane, HCM shows the highest FRR than that of MCM and HCM. It could be due to lower relative roughness of the membrane surface as evidenced by SEM images. The lower surface roughness results in easier hydraulic cleaning. The fouling ratio evaluation also shows that unmodified membrane has highest total fouling ratio. According to the fouling ratio profile, the fouling mechanism that occurred in the membranes in this study are the combination of pore blocking and cake filtration. From the Figure 7 reveals that reversible fouling is higher than irreversible fouling. It indicates that oil droplet was deposited on the membrane surface. With the chitosan coating, the reversible fouling ratio relative to irreversible fouling ratio has decreased significantly. It proves that the presence of chitosan layer prevents the pore blocking by proving hydrophilic layer and denser skin layer of the prepared ceramic membrane. The excellent antifouling performance of the modified ceramic membranes may be attributed to the two factors. One is that a large number of hydroxyl groups in the surface of membranes resulted from location of the chitosan coating in the surface of the prepared membranes. Another is that by addition of the chitosan on the fly ash/kaolin ceramic membrane, the surface of the resulted membranes has been smoother rather than the unmodified membrane. The fouling ratio of HCM is higher than LCM and MCM. The most influencing factor is membrane surface roughness, the HCM has higher rheological properties which is leading on the rougher membrane formation during coagulation process. The results from above studies suggested that the newly fabricated ceramic membranes by chitosan coating, which had lower fouling and higher oil rejection related to the unmodified membrane, could be used as a suitable membrane in the filtration of industrial effluents and treatment of wastewaters.

CONCLUSION

Chitosan modified fly ash/kaolin ceramic membrane has been successfully fabricated via simple surface coating procedure. In this paper, fly ash/kaolin was prepared via sintering process and followed by surface coating of chitosan with different molecular weight. The SEM characterization showed that the HCM shows the denser membrane surface due to the highest polymer packing density of chitosan. It helps in rejecting the pollutant during filtration experiment. The TGA analysis also shows that the membrane has excellent thermal stability indicated by insignificant mass losses. The XRD analysis revealed the conversion of kaolinite to mullite due to sintering process that increase the density of the ceramic membrane. it also confirmed that the chitosan coating insignificantly changes the membrane structural phases. The chemical composition evaluation via FTIR has also revealed the hydrophilic groups that beneficial for fouling mitigation. The best pore structure was obtained by HCM membrane with porosity of 49.71% and pore size radius of 15 nm. Among the three prepared membranes (LCM, MCM, and HCM), the HCM membrane has shown the most favored characteristic and performance. The HCM also showed steady permeate fluxes indicating the enhanced antifouling properties. The oil rejection was also enhanced up to 99.8% by high molecular weight chitosan coating. Regarding the obtained membrane characteristics and performances, the best membrane was achieved by HCM membrane with high oil rejection with moderate permeate flux which may lead to new application of membrane for oily wastewater treatment.

REFERENCES

Agarwal, A., Samanta, A., Nandi, B. K., & Mandal, A. (2020). Synthesis, characterization and performance studies of kaolin-fly ash-based membranes for microfiltration of oily waste water. Journal of Petroleum Science and Engineering, 194, 107475.

Al-Thani, R. F., & Yasseen, B. T. (2020). Phytoremediation of polluted soils and waters by native Qatari plants: Future perspectives. Environmental Pollution, 259, 113694.

Apriyanti, E., Hadiyanto, & Wijayanto, W. (2018). Preparation and Characterization of Volcanic Ash-chitosan Composite Ceramic Membrane for Clean Water Production. Journal of Environmental Science and Technology, 11(3), pp. 112–118.

Bakare, B. F., & Adeyinka, G. C. (2022). Evaluating the Potential Health Risks of Selected Heavy Metals

across Four Wastewater Treatment Water Works in Durban, South Africa. Toxics, 10(6), pp. 340.

Bat-Amgalan, M., Miyamoto, N., Kano, N., Yunden, G., & Kim, H.-J. (2022). Preparation and Characterization of Low-Cost Ceramic Membrane Coated with Chitosan: Application to the Ultrafine Filtration of Cr(VI). Membranes, 12(9), pp. 835.

Bousbih, S., Errais, E., Darragi, F., Duplay, J., Trabelsi-Ayadi, M., Daramola, M. O., & Ben Amar, R. (2021). Treatment of textile wastewater using monolayered ultrafiltation ceramic membrane fabricated from natural kaolin clay. Environmental Technology, 42(21), pp. 3348–3359.

Chen, M., Heijman, S. G. J., & Rietveld, L. C. (2021). State-of-the-Art Ceramic Membranes for Oily Wastewater Treatment: Modification and Application. Membranes, 11(11), Article 11.

Das, D., Nijhuma, K., Gabriel, A. M., Daniel, G. P. F., & Murilo, D. de M. I. (2020). Recycling of coal fly ash for fabrication of elongated mullite rod bonded porous SiC ceramic membrane and its application in filtration. Journal of the European Ceramic Society, 40(5), pp. 2163–2172.

Dereszewska, A., Cytawa, S., Tomczak-Wandzel, R., & Medrzycka, K. (2015). The Effect of Anionic Surfactant Concentration on Activated Sludge Condition and Phosphate Release in Biological Treatment Plant. Polish Journal of Environmental Studies, 24, pp. 83–91.

Dong, Y., Wu, H., Yang, F., & Gray, S. (2022). Cost and efficiency perspectives of ceramic membranes for water treatment. Water Research, 220, 118629.

Drozdova, J., Raclavska, H., Raclavsky, K., & Skrobankova, H. (2019). Heavy metals in domestic wastewater with respect to urban population in Ostrava, Czech Republic. Water and Environment Journal, 33(1), pp. 77–85.

Eljaiek-Urzola, M., Romero-Sierra, N., Segrera-Cabarcas, L., Valdelamar-Martínez, D., & Quiñones-Bolaños, É. (2019). Oil and Grease as a Water Quality Index Parameter for the Conservation of Marine Biota. Water, 11(4), 856.

Ghanbari, M., Esmaeilzadeh, F., & Binazadeh, M. (2018). An experimental investigation of creaming phenomenon using a novel optical method: A case study of mineral oil-in-water emulsion. Journal of Dispersion Science and Technology, 39(5), 634–643. https://doi.org/10.1080/01932691.2017.1379019

Guo, R., Ma, X., Hu, C., & Jiang, Z. (2007). Novel PVA–silica nanocomposite membrane for pervaporative dehydration of ethylene glycol aqueous solution. Polymer, 48(10), 2939–2945. https://doi.org/10.1016/j.polymer.2007.03.035

He, X., & Li, P. (2020). Surface Water Pollution in the Middle Chinese Loess Plateau with Special Focus on Hexavalent Chromium (Cr6+): Occurrence, Sources and Health Risks. Exposure and Health, 12(3), 385–401. https://doi.org/10.1007/s12403-020-00344-x

Hubadillah, S. K., Harun, Z., Othman, M. H. D., Ismail, A. F., & Gani, P. (2016). Effect of kaolin particle size and loading on the characteristics of kaolin ceramic support prepared via phase inversion technique. Journal of Asian Ceramic Societies, 4(2), 164–177. https://doi.org/10.1016/j.jascer.2016.02.002

Hubadillah, S. K., Jamalludin, M. R., Othman, M. H. D., & Adam, M. R. (2023). A novel bio-ceramic hollow fibre membrane-based hydroxyapatite derived from Tilapia fish bone for hybrid arsenic separation/adsorption from water. Materials Today: Proceedings.
https://doi.org/10.1016/j.matpr.2022.12.232

Jafari, B., Rezaei, E., Dianat, M. J., Abbasi, M., Hashemifard, S. A., Khosravi, A., & Sillanpää, M. (2021). Development of a new composite ceramic membrane from mullite, silicon carbide and activated carbon for treating greywater. Ceramics International, 47(24), 34667–34675. https://doi.org/10.1016/j.ceramint.2021.09.005

Kadam, A., Wagh, V., Umrikar, B., & Sankhua, R. (2020). An implication of boron and fluoride contamination and its exposure risk in groundwater resources in semi-arid region, Western India. Environment, Development and Sustainability, 22(7), 7033–7056. https://doi.org/10.1007/s10668-019-00527-w

Kapadnis, G., Dey, A., Dandekar, P., & Jain, R. (2019). Effect of degree of deacetylation on solubility of low-molecular-weight chitosan produced via enzymatic breakdown of chitosan. Polymer International, 68(6), 1054–1063. https://doi.org/10.1002/pi.5795

Khozanah, Yogaswara, D., & Wulandari, I. (2021). Oil and Grease (OG) Content in Seawater and Sediment of The Jakarta Bay and its Surrounding. IOP Conference Series: Earth and Environmental Science, 789(1), 012015. https://doi.org/10.1088/1755-1315/789/1/012015

Kotobuki, M., Gu, Q., Zhang, L., & Wang, J. (2021). Ceramic-Polymer Composite Membranes for Water and Wastewater Treatment: Bridging the Big Gap between Ceramics and Polymers. Molecules, 26(11), 3331.

Kusworo, T. D., Ismail, A. F., Aryanti, N., Widayat, W., Qudratun, Q., & Utomo, D. P. (2017). Enhanced Anti-Fouling Behavior and Performances of Nano Hybrid Pes-Sio2 And Pes-Zno Membranes For Produced Water Treatment. Jurnal Teknologi, 79(6), pp. 129-140.

Kusworo, T. D., Kumoro, A. C., Utomo, D. P., Kusumah, F. M., & Pratiwi, M. D. (2021). Performance of the Crosslinked PVA Coated PES-TiO2 Nano Hybrid Membrane for the Treatment of Pretreated Natural Rubber Wastewater Involving Sequential Adsorption – Ozonation Processes. Journal of Environmental Chemical Engineering, 9(2), 104855.

Kyriakogona, K., Giannopoulou, I., & Panias, D. (2017, June). Extraction of Aluminium from Kaolin: A Comparative Study of Hydrometallurgical Processes. The 3rd World Congress on Mechanical, Chemical, and Material Engineering. pp. 133-1 – 133-6.

Li, C., Sun, W., Lu, Z., Ao, X., Yang, C., & Li, S. (2019). Systematic evaluation of TiO2-GO-modified ceramic membranes for water treatment: Retention properties and fouling mechanisms. Chemical Engineering Journal, 378, 122138.

Li, Y., Li, H., Xu, X., Xiao, S., Wang, S., & Xu, S. (2017). Fate of nitrogen in subsurface infiltration system for treating secondary effluent. Water Science and Engineering, 10(3), pp. 217–224.

Liu, G., Yang, Y., Liu, H., Wang, Q., Wang, Y., Zhou, J., & Chang, Q. (2023). Preparation of disc ceramic membrane by a printing and dip-coating method for oil-water separation. Separation and Purification Technology, 315, 123552.

Mouiya, M., Bouazizi, A., Abourriche, A., Benhammou, A., El Hafiane, Y., Ouammou, M., Abouliatim, Y., Younssi, S. A., Smith, A., & Hannache, H. (2019). Fabrication and characterization of a ceramic membrane from clay and banana peel powder: Application to industrial wastewater treatment. Materials Chemistry and Physics, 227, pp. 291–301.

Pastore, C., Pagano, M., Lopez, A., Mininni, G., & Mascolo, G. (2015). Fat, oil and grease waste from municipal wastewater: Characterization, activation and sustainable conversion into biofuel. Water Science and Technology, 71(8), pp. 1151–1157.

Saini, P., Bulasara, V. K., & Reddy, A. S. (2019). Performance of a new ceramic microfiltration membrane based on kaolin in textile industry wastewater treatment. Chemical Engineering Communications, 206(2), pp. 227–236.

Siskens, C. A. M. (1996). Chapter 13 Applications of ceramic membranes in liquid filtration. In A. J. Burggraaf & L. Cot (Eds.), Membrane Science and Technology. 4, pp. 619–639.

Widyarani, Wulan, D. R., Hamidah, U., Komarulzaman, A., Rosmalina, R. T., & Sintawardani, N. (2022). Domestic wastewater in Indonesia: Generation, characteristics and treatment. Environmental Science and Pollution Research, 29(22), pp. 32397–32414